

Mutations in *orbit/mast* reveal that the central spindle is comprised of two microtubule populations, those that initiate cleavage and those that propagate furrow ingression

Yoshihiro H. Inoue,¹ Matthew S. Savoian,² Takao Suzuki,¹ Endre Máthé,² Masa-Toshi Yamamoto,¹ and David M. Glover²

¹Drosophila Genetic Resource Center, Kyoto Institute of Technology, Kyoto 616-8354, Japan

²Cancer Research UK Cell Cycle Genetics Research Group, Department of Genetics, University of Cambridge, Cambridge CB2 3EH, England, UK

We address the relative roles of astral and central spindle microtubules (MTs) in cytokinesis of *Drosophila melanogaster* primary spermatocytes. Time-lapse imaging studies reveal that the central spindle is comprised of two MT populations, “interior” central spindle MTs found within the spindle envelope and “peripheral” astral MTs that probe the cytoplasm and initiate cleavage furrows where they contact the cortex and form overlapping bundles. The MT-associated protein Orbit/Mast/CLASP concentrates on interior rather than peripheral central

spindle MTs. Interior MTs are preferentially affected in hypomorphic *orbit* mutants, and consequently the interior central spindle fails to form or is unstable. In contrast, peripheral MTs still probe the cortex and form regions of overlap that recruit the Pav-KLP motor and Aurora B kinase. *orbit* mutants have disorganized or incomplete anillin and actin rings, and although cleavage furrows initiate, they ultimately regress. Our work identifies a new function for Orbit/Mast/CLASP and identifies a novel MT population involved in cleavage furrow initiation.

Introduction

The terminal event of cell division, cytokinesis, is driven by the constriction of an actomyosin “contractile” ring (Satterwhite and Pollard, 1992). However, the mechanisms responsible for determining the cleavage site remain poorly understood. Data from a variety of systems have implicated the spindle, a bipolar microtubule (MT) structure, in dictating furrow position (Field et al., 1999). Three models have been put forward to explain how the spindle and its component MTs might signal furrow formation. The first is exemplified from experiments in which cells containing multiple spindles enter cytokinesis. In systems as diverse as echinoderm eggs (Rappaport, 1961) and cultured vertebrate somatic cells (Eckley et al., 1997; Rieder et al., 1997; Savoian et al.,

1999), cleavage furrows initiate at the spindle equators as expected, as well as between the adjacent spindles. These observations raised the possibility that astral MTs provide a positive signal for furrow positioning and induction. In contrast, a second model suggests a negative regulatory role for astral MTs (Wolpert, 1960). Here, the polar regions of a cell would be less contractile due to the higher density of astral MTs. In agreement with this finding, Dechant and Glotzer (2003) noted that in *Caenorhabditis elegans* embryos, furrows initiate at locations where the MT density is lowest. A third model, that accommodates physical and genetic data, attributes furrow positioning to the central spindle, a dense array of overlapping MTs that forms during late anaphase. For example, placement of a barrier between one side of the central spindle and the cell cortex results in furrow formation only on the nonobstructed side (Cao and Wang, 1996). Gatti et al. (2000) have shown that the central spindle is necessary and sufficient for furrow formation in *Drosoph-*

Y.H. Inoue and M.S. Savoian contributed equally to this paper.

The online version of this article includes supplemental material.

Address correspondence to Y.H. Inoue, Drosophila Genetic Resource Center, Kyoto Institute of Technology, Sagaippongi-cho, Ukyou-ku, Kyoto 616-8354, Japan. Tel.: 81-75-873-2653. Fax: 81-75-861-0881. email: yhinoue@ipc.kit.ac.jp

Key words: cytokinesis; *Drosophila*; meiosis; MAP; CLASP

Abbreviations used in this paper: DIC, differential interference contrast; MAP, MT-associated protein; MT, microtubule.

ila melanogaster cells. Mutations that greatly diminish astral MTs without apparently affecting the central spindle do not inhibit cytokinesis as revealed by fixed meiotic (Bonaccorsi et al., 1998) and mitotic (Giansanti et al., 2001) cells. Furthermore, loss of central spindle integrity by mutation or RNAi leads to polyploid cells (Adams et al., 1998; Somma et al., 2002). Several studies in *C. elegans* embryos have shown that the central spindle is dispensable for furrow initiation but is involved in its propagation for midbody formation (Powers et al., 1998; Raich et al., 1998; Jantsch-Plunger et al., 2000). Interestingly, when anaphase B spindle elongation is genetically restricted in these cells, a dependence on the central spindle for furrow initiation is observed (Dechant and Glotzer, 2003). Thus, the roles that the different MTs serve in cytokinesis remains unclear.

We have begun to approach this problem by examining the effects of mutations on a variety of MT-associated proteins (MAPs) during the onset of cytokinesis in *Drosophila* primary spermatocytes. Here we examine the role of the Orbit/Mast protein. *Drosophila orbit/mast* mutants were first identified through genetic screens as displaying a variety of mitotic defects including the formation of both mono- and multipolar spindles (Inoue et al., 2000; Lemos et al., 2000). Time-lapse observations of *mast* mutant embryos supported by RNAi studies on cultured cells showed that the gene product was needed to maintain spindle bipolarity and chromosome congression (Maiato et al., 2002). The Orbit/Mast protein has its counterpart in mammalian cells in the form of the CLASPs, two related proteins identified through their ability to interact with CLIP-170/CLIP-115 proteins that associate with MT plus ends (Akhmanova et al., 2001).

A recent study of the mitotic role of CLASP1 using antibody microinjection into cultured mammalian cells revealed a similar phenotype to that seen following RNAi of Orbit/Mast in *Drosophila* S2 cells (Maiato et al., 2002, 2003). Monopolar spindles formed in which the chromosomes became buried in the interior of the monoaster. In both cases, treatment with MT stabilizing drugs caused the chromosomes to move to the plus ends of the MTs at the astral periphery. This finding was interpreted to indicate a role in regulating MT dynamics, specifically the transition from shrinkage to growth of the kinetochore MTs that link each chromosome to the spindle. The localization of both Orbit/Mast and CLASPs to the kinetochore is consistent with the above postulated role. Orbit/Mast also associates with the central region of late mitotic spindles in both *Drosophila* and mammalian cells (Inoue et al., 2000; Lemos et al., 2000; Maiato et al., 2003), as well as the ring canals and fusome of oocytes (Máthé et al., 2003). However, the metaphase arrest associated with the aforementioned spindle and chromosome congression defects has prevented the roles of Orbit/Mast during cytokinesis from being determined.

Here, we provide the first characterization of central spindle formation in living *Drosophila* primary spermatocytes. We find that the central spindle consists of two distinct sets of MTs, “peripheral” astral MTs and “interior” MTs that are confined within the spindle envelope, the highly fenestrated remains of the nuclear membrane that persist in *Drosophila* cells (Tates, 1971; Stafstrom and Staehelin, 1984). These MT populations appear biochemically distinct as they show

a differential association with the MAP encoded by *orbit/mast*. Time-lapse imaging reveals that the future cleavage site corresponds to locations where peripheral MTs contact the cortex and then bundle together. Furrows initiate and ingress, thereby coalescing peripheral and interior MTs to consolidate the late central spindle. The weak metaphase spindle integrity checkpoint in *Drosophila* primary spermatocytes (Rebollo and Gonzalez, 2000; Savoian et al., 2000) provides the opportunity to examine late division events in mutants that would normally undergo metaphase arrest in the mitotic cells of somatic tissues (e.g., Polo kinase and Asp; Carmena et al., 1998; Wakefield et al., 2001; Riparbelli et al., 2002). We find that in hypomorphic *orbit* mutants, peripheral MTs still contact the cortex and bundle, but interior MTs often fail to organize or are unstable and cleavage fails. In agreement with this phenotype, we show that in wild-type cells the Orbit/Mast protein concentrates on the spindle, but after anaphase onset selectively accumulates in the region described as the spindle matrix (Scholey et al., 2001), which is occupied by interior but not peripheral MT bundles.

Results

Central spindles are comprised of two MT populations, peripheral and interior

The ongoing debate about the relative contribution of astral and central spindle MTs in the positioning of the cleavage furrow led us to examine the dynamics of MT behavior in living *Drosophila* primary spermatocytes. To this end, we used a transgenic line ubiquitously expressing EGFP-tagged β -tubulin. We followed these otherwise wild-type cells (Fig. S1 and Table S1, available at <http://www.jcb.org/cgi/content/full/jcb.200402052/DC1>) by multidimensional, near simultaneous, differential interference contrast (DIC) and fluorescence, time-lapse microscopy (Fig. 1 and Video 1, available at <http://www.jcb.org/cgi/content/full/jcb.200402052/DC1>). Before anaphase onset (Fig. 1, -1 min), the polar regions of the cytoplasm contained numerous astral MTs, some of which appeared to be separated from the centrosomes. We found that the post-anaphase spindle contained two distinct populations of MTs (Fig. 1, 5 min), a peripheral set (Fig. 1, p) of long astral MTs originating from the polar regions of the cell, which became more robust and dynamic as they “probed” the cytoplasm reaching toward the equator (Fig. 1, 5 min, open arrowheads), and an interior set (Fig. 1, i) found within the remnants of the nuclear envelope, which appeared to elongate from the spindle poles, but did not extend into the equatorial region (Fig. 1, 5 min, closed arrowheads). Shortly thereafter, the peripheral MTs formed protrusions that contacted the cortex and formed bundles (Fig. 1, 8 min, open arrows). The interior and most of the peripheral MTs then appeared to be released and translocated to the spindle equator, leaving behind a denuded area at the polar regions (Fig. 1, closed arrowheads, 10 min and accentuated at 12 min). The release of interior MTs from the poles and their concentration at the equator can also be seen in the linescan plots of pixel intensity taken along the spindle axis (Fig. 1, white line and graphic in insets at 5–12 min, the centrosomes are denoted

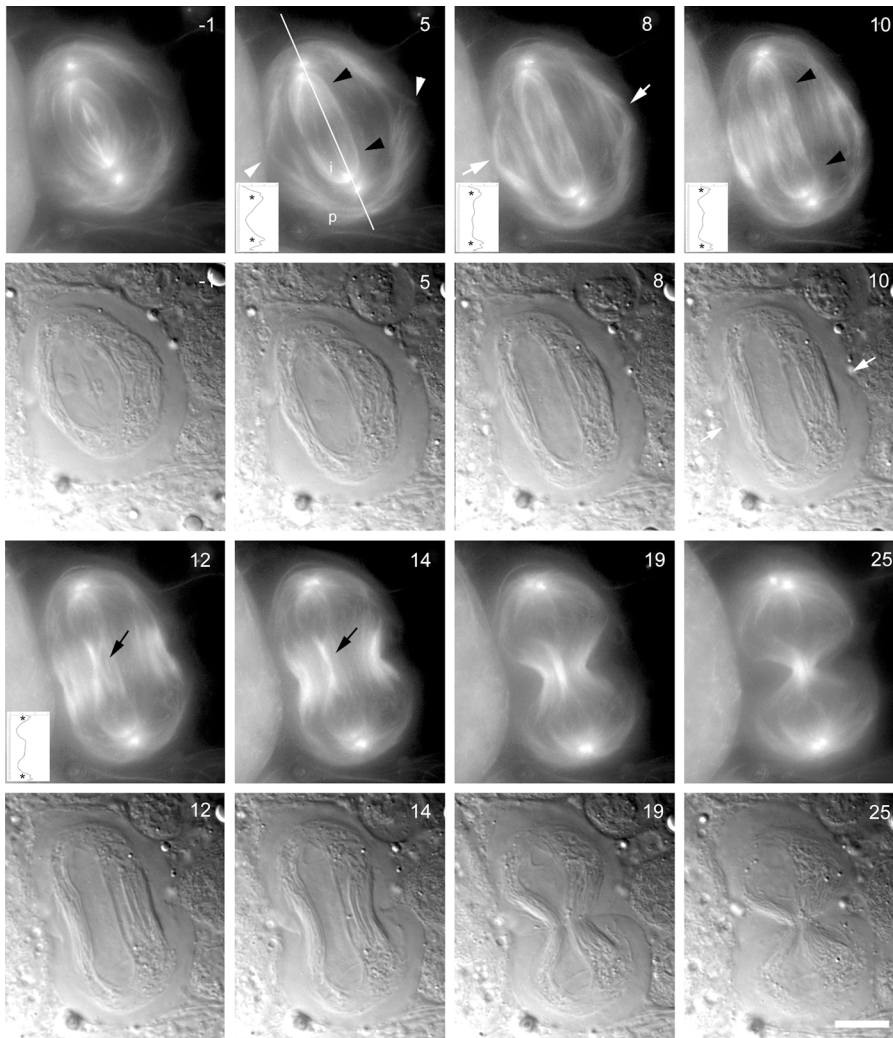


Figure 1. Dynamics of central spindle formation in wild-type primary spermatocytes. Selected frames from a time-lapse sequence of a β -tubulin-EGFP-expressing cell during cytokinesis showing the distribution of MTs (top) and the corresponding DIC images to reveal the positions of the chromosomes and the cell cortex. Time in each panel is in minutes relative to anaphase onset. The astral MTs cap the ends of the spindle, but some MTs only appear loosely associated with the centrosomes. Some of these peripheral (p) MTs become more robust and dynamic and run along the cell periphery and probe the cytoplasm (5 min, open arrowheads). At this time, the MTs found inside of the remnants of the nuclear envelope, the interior (i) MTs, appear to elongate from the spindle poles, but do not extend into the equator (closed arrowheads). Shortly thereafter, the peripheral MTs contact the cortex and bundle together forming protrusions that continue their cortical association (8 min, open arrows). The interior MTs as well as most of the peripheral MTs appear to be released from the polar regions and translocate to the spindle equator (closed arrowheads; 10 min). As cytokinesis initiates (10 min, DIC panel, open arrows), the interior MTs become bundled irrespective of the degree to which the cytoplasm has constricted (e.g., closed arrows at 12 and 14 min). Propagation of the cleavage furrow ultimately compacts both peripheral and interior MT bundles into a common central spindle (19 min) and subsequent midbody (25 min). The distribution of the interior MTs can also be followed by comparing the linescan fluorescence intensity plots (insets; 5–12 min, asterisks indicate the centrosomes) taken along the spindle long axis as shown by the white line in 5 min. Bar, 10 μ m.

by the asterisks). Concomitantly (Fig. 1, 12 and 14 min) the peripheral and interior (Fig. 1, closed arrows) MTs formed independent bundles at the equator appearing as a broad central spindle. Cleavage initiated 9 ± 1 min after anaphase onset ($n = 10$), after the peripheral MTs from the two poles had contacted the cell cortex (Fig. 1, 10 min, open arrows). These peripheral- and interior-central spindle MT bundles ultimately compacted into a common midbody as the cleavage furrow ingressed (Fig. 1, 19–25 min).

The dynamics by which peripheral MTs emanating from each pole contact the equatorial cortex before furrow ingression is clearly illustrated in the wild-type cell in Fig. 2 (Video 2, available at <http://www.jcb.org/cgi/content/full/jcb.200402052/DC1>). This particular cell was distended at its equator such that the peripheral MTs had to probe some 20 μ m into the cytoplasm (Fig. 2, 2 min, closed arrowhead) before they made cortical contact (Fig. 2, 4 min) and then became bundled (Fig. 2, 7 min) at the future cleavage site. In this cell, as with all of the others we observed, furrows initiated ~ 1 min after peripheral MT bundles became visible

and proceeded until the peripheral central spindle MT bundles came to lie alongside the interior ones (Fig. 2, 12–17 min).

To confirm that this probing behavior was not specific to meiotic cells, we extended our time-lapse analyses to mitotic S2 cells expressing tubulin tagged with GFP (Goshima and Vale, 2003). Consistent with the aforementioned results, we observed long peripheral astral MTs contacting the cleavage site shortly before or concomitant with furrow initiation ($n = 5$; Fig. S2 and Video 3, available at <http://www.jcb.org/cgi/content/full/jcb.200402052/DC1>). Therefore, cortical contact by peripheral MTs at the future cleavage site is a conserved feature of cytokinesis.

Orbit/Mast associates with spindle MTs and concentrates at interior but not peripheral regions of the cell

Previous studies had shown that the Orbit/Mast protein localized to mitotic central spindles in late anaphase. We wished to determine if this was also the case in male meiosis I and if the protein might show selective distribution on the

Figure 2. Cleavage furrows initiate at the cortical contact site of opposing peripheral central spindle MTs. Selected frames from a time-lapse sequence of a cell with a displaced spindle (–1 min). The subsequent panels show a higher magnification view of the boxed region. After anaphase onset, the peripheral MTs (arrowheads) extend through the cytoplasm until they approach the cortex. They continue to probe (2 min) until cortical contact is made (4 min), at which time they become bundled (7 min). Shortly thereafter, the cleavage furrow initiates and ingresses, thereby coalescing peripheral and interior MTs (12 and 17 min). The fluorescence signal has been inverted to allow more details to be observed. Time is in minutes relative to anaphase onset. Bars, 10 μ m.

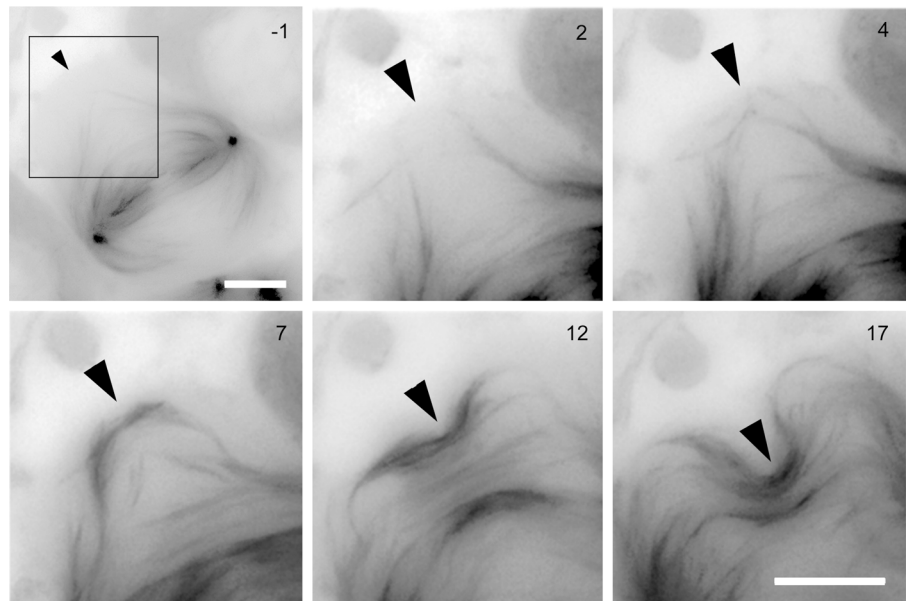
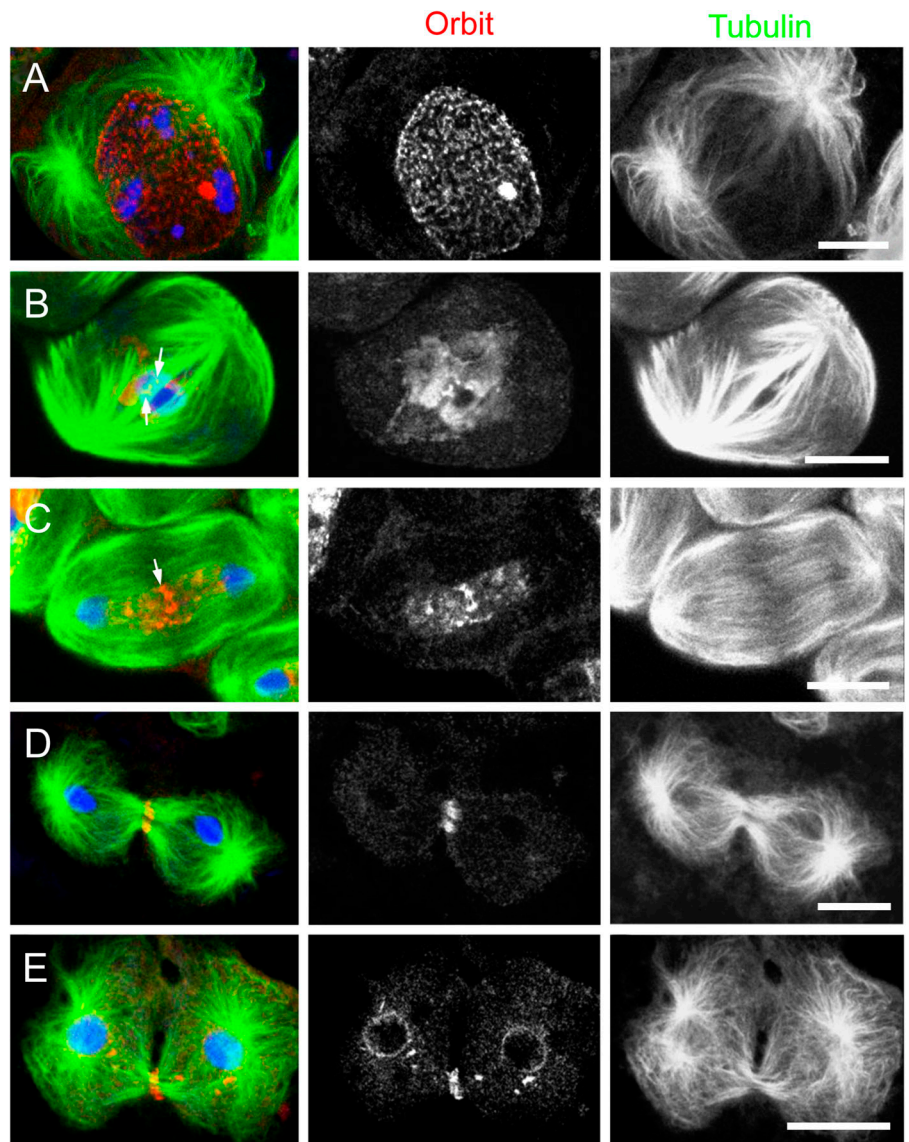


Figure 3. Localization of Orbit/Mast protein in primary spermatocytes. (left) Wild-type spermatocytes stained to reveal Orbit/Mast (red), MTs (green), and DNA (blue). The individual Orbit/Mast and MT distributions are also shown. (A) During prophase, Orbit/Mast is associated with the nuclear membrane, throughout the nucleus, and on specific regions of chromatin. (B) At prometaphase/metaphase, it remains predominantly within the putative spindle envelope in the spindle matrix region and forms chromatin proximal spots that may be kinetochores or MT plus ends (arrows). (C) During anaphase, Orbit/Mast remains concentrated in the region corresponding to the spindle matrix that contains the interior central spindle MTs, and begins to form aggregates (arrow) at the spindle equator. It does not appear to concentrate in locations occupied by the peripheral MTs. (D) By telophase, the protein accumulates on the mid-part of the central spindle, where it remains as cleavage continues. (E) In these later stages, Orbit/Mast can also be detected on the peripheries of the reforming karyomeres. Bars, 10 μ m.



different subsets of MTs. Immunostaining revealed that in prophase, the protein had a predominantly punctate distribution within the nucleus, with a lower level of staining in the cytoplasm in an area not occupied by the asters (Fig. 3 A). During prometaphase/metaphase, Orbit/Mast concentrated on spindle MTs and also formed aggregates near the chromosomes, which may be kinetochores or MT plus ends (Fig. 3 B, arrows) as previously reported (Maiato et al., 2003). Interestingly, the protein did not strongly accumulate at the asters. At late anaphase, the staining became more granular but remained confined to the putative spindle matrix and the region occupied by the interior spindle MTs. Orbit/Mast also aggregated at the mid-point of the nascent interior central spindle (Fig. 3 C, arrow). Notably, the protein did not concentrate at higher than background levels on peripheral central spindle MTs. By telophase, most of the protein was concentrated at the mid-zone of the combined peripheral and interior central spindle MTs (Fig. 3 D). As cleavage progressed Orbit/Mast remained in this region but also showed a diffuse distribution throughout the cytoplasm and an association with the nuclear peripheries in the daughter cells (Fig. 3 E). Thus, Orbit/Mast more strongly accumulates in the interior than the peripheral regions of the cell during central spindle formation.

Cytokinesis fails in *orbit* mutants

The distribution of Orbit/Mast may indicate functions not only in karyokinesis but also in cytokinesis. Therefore, we wished to study the male meiotic divisions in *orbit* mutants. Male meiosis allows the viewing of mutant phenotypes in the later stages of cell division that are masked in somatic cells by the more robust spindle integrity checkpoint (Introduction). Initial attempts to study cytokinesis using the previously described *orbit* alleles *orbit¹* and *orbit⁵* proved unsuccessful, as testes from the former were aberrant and diminutive (Fig. S1) and the latter were so defect ridden as to lack spermatids entirely. Therefore, we chose to study cytokinesis using two new, weak hypomorphic alleles, *orbit⁷* and *orbit⁸*, the products of an imprecise excision generated through the remobilization of the *orbit⁵* P-element (Máthé et al., 2003).

We began our analysis of the new hypomorphic mutants by examining post-meiotic onion stage spermatids. Each wild-type spermatid contains a single phase lucent nucleus and a similarly sized phase dense mitochondrial derivative, the Nebenkern (Fig. 4 A). In *orbit⁷* mutants (Fig. 4 B), the spermatids contained irregularly sized nuclei (arrows) or multiple nuclei and an enlarged Nebenkern (arrowhead). These abnormalities reveal defects in karyokinesis and cytokinesis, respectively. *orbit⁸* mutants had a similar phenotype with spermatids containing increased numbers of nuclei and correspondingly enlarged Nebenkern (Fig. 4 C). The phenotypes could be fully rescued through a wild-type transgene, indicating that the defects were the direct result of a lesion in the *orbit* gene. Surprisingly, the two mutants only show slightly diminished protein levels by Western blot (Fig. 4 D). Consistent with the presence of Orbit/Mast protein on the interior central spindle MTs in wild-type spermatocytes, weak hypomorphic mutant alleles of *orbit* display cytokinesis defects. Indeed, we found that fixed preparations

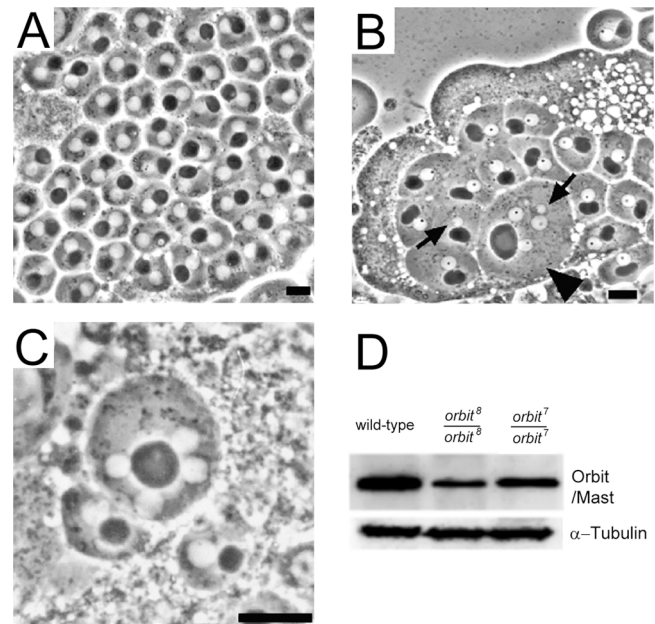


Figure 4. Defects in karyokinesis and cytokinesis in *orbit* mutants. Living spermatids at post-meiotic onion stage were examined by phase-contrast microscopy for defects in cytokinesis. (A) Wild-type cyst. (B) part of an onion stage cyst from *orbit⁷*. The arrows reveal abnormally sized nuclei, indicative of karyokinetic defects. In one such cell (arrowhead), five nuclei are present along with an enlarged Nebenkern, revealing defects during karyokinesis and cytokinesis. (C) Binucleate spermatid from *orbit⁸*. Note the similar defects to those seen in B. (D) Western blots of extracts prepared from wild-type or mutant adult testes. α -Tubulin has been used as a protein loading control. Bars, 10 μ m.

of *orbit* spermatocytes had aberrant central spindles (Table I and see Figs. 6–8).

Cleavage furrows initiate in *orbit* mutants but regress in the absence of stable interior central spindles

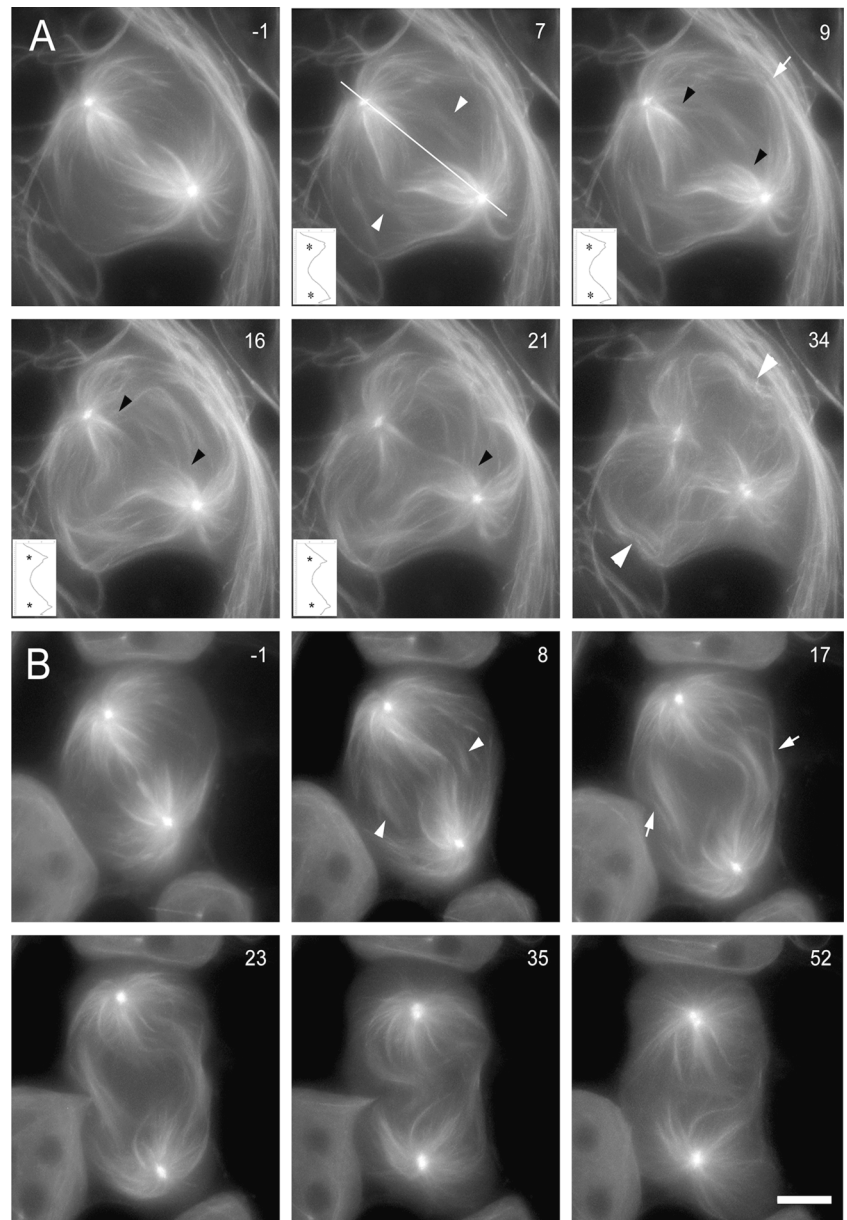
To observe the behavior of MTs in living spermatocytes with diminished levels of Orbit, we introduced the EGFP-tagged β -tubulin gene into the *orbit⁷* line. As expected in such a hypomorphic allele, we observed many normal cells by time-lapse analysis. Of the 15 cells followed, 40% (6/15) exhibited no obvious abnormalities, whereas the remaining nine cells exhibited cleavage defects. Fig. 5 shows selected frames from time-lapse sequences of primary spermatocytes from this line during cytokinesis. In the top cell (Fig. 5 A and Video 4, available at <http://www.jcb.org/cgi/content/>

Table I. Central spindle defects in *orbit⁷* mutants

Genotype	n	Central Spindle (CS) Status			Abnormal CS	%
		Normal CS	Peripheral CS present but interior CS absent	Both peripheral and interior CS absent		
<i>orbit⁷/orbit⁷</i>	123	84	26	13	32	
β -tubulin-EGFP/ β -tubulin-EGFP	76	75	1	0	1	

CS, central spindle.

Figure 5. Loss of *orbit* preferentially affects interior but not peripheral MTs. (A and B) Selected frames from time-lapse recordings of *orbit*⁷ primary spermatocytes expressing β -tubulin-EGFP undergoing cytokinesis. (A) After anaphase onset (0 min time point; not depicted), astral MTs probe the cytoplasm (7 min) until contacting the cortex where they form bundles (9 min, arrow). Peripheral MTs can be detected (e.g., 7 min, arrowheads) in the cytoplasm around the spindle, although not as densely arranged as in control cells. In this cell, no furrow ingression was observed until the 34 min time point (arrowheads). During the intervening period, the interior MTs associated with each half spindle (9–21 min, arrowheads) remained associated with the spindle poles and did not appear to release and translocate to the equator (see also linescan insets; asterisks indicate the centrosomes). The spindle then collapsed upon itself. (B) Another example of cytokinesis in an *orbit* mutant. The peripheral MTs in this cell appear less dynamic than in the wild-type. They probe the cytoplasm (8 min) and ultimately form feeble peripheral bundles (17 min, arrows). During this time, the more interiorly positioned peripheral MTs form bundles that are abnormally robust relative to those adjacent to the cortex (8 min, arrowheads). As the cleavage furrow forms and ingresses, cytoplasmic and cortically proximal peripheral MT bundles contact one another (23 min). Furrow ingression abruptly arrests on the right hand side of the cell but continues on the left. This unilateral furrow advances before also halting and then ultimately regressing (35 min). Note how the region within the spindle envelope lacks any ostensible interior central spindle. Few interior MTs could be detected during the course of filming and those appeared to rapidly degrade. All times are in minutes relative to anaphase onset. Bar, 10 μ m.



full/jcb.200402052/DC1), the anaphase peripheral MTs probed the cytoplasm toward the equator similar to our observations of wild-type cells (Fig. 5 A, 7 min). These peripheral MTs then contacted the cortex (Fig. 5 A, arrow at 9 min) where they formed distinct bundles that appeared diminished relative to control cells (Fig. 5 A, 16 min). Other peripheral MTs were also detected (Fig. 5 A, 7 min, arrowheads) in the cytoplasm that enshrouded the interior spindle and increased in robustness throughout the course of filming. Furrow ingression was greatly delayed (Fig. 5 A, 34 min, arrowheads) but still initiated at the site where the bundles of peripheral MTs contacted the cortex. During this course of time, the interior MTs found in each half spindle (Fig. 5 A, 9–21 min, closed arrowheads) appeared to remain associated with their respective spindle poles. They did not release and translocate away from the poles or otherwise extend into the equatorial region (this can also be seen in the linescan insets of fluorescence intensity taken along the axis

shown in at the 7-min time point). The spindle in this particular cell subsequently collapsed and cytokinesis failed.

Another example of cytokinesis in an *orbit*⁷ mutant cell is shown in Fig. 5 B (Video 5, available at <http://www.jcb.org/cgi/content/full/jcb.200402052/DC1>). As expected, the peripheral MTs of this cell probed the cytoplasm, but only formed very feeble bundles (Fig. 5 B, 17 min, arrows). Also visible is a concentration of peripheral MTs that are adjacent to the spindle (Fig. 5, 8 min, arrowheads), which appear abnormally robust relative to the diminished MTs near the cortex. We found that 73% ($n = 15$) of the *orbit*⁷ mutant cells analyzed formed normal peripheral MT bundles. The remaining 27% of the cells exhibited abnormalities that manifest as an apparent decrease in MT probing or, more often, as a reduction in the robustness of the peripheral MT bundles and an instability leading to degradation before cleavage. Despite such a diminution in mutants, peripheral MTs still contacted the cortex and cytoplasmic constriction initiated. In

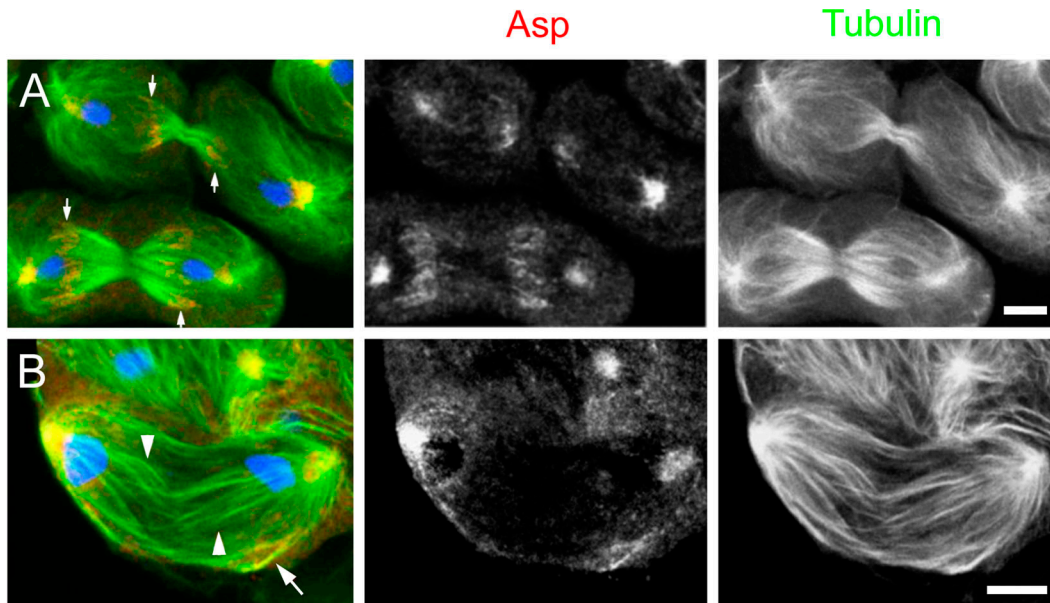


Figure 6. **Asp staining reveals MTs fail to detach from the spindle poles for central spindle formation in *orbit* spermatocytes.** (left) Localization of Asp (red), MTs (green), and DNA (blue) in wild-type (A) and *orbit* mutant (B) testes. (A) In wild-type spermatocytes, Asp localizes to spindle poles and along the minus ends of the central spindle MTs (arrows) at late anaphase and telophase. (B) In *orbit* mutant cells in which the interior central spindle does not form, Asp remains primarily associated with the centrosomes and spindle poles. It is undetectable at the predicted location of the interior central spindle (arrowheads). In those cases where peripheral central spindle MTs are apparent, Asp has the expected distribution on presumptive MT minus ends (arrow). Bars, 5 μ m.

the cell shown in Fig. 5 B the furrow initiated in a symmetrical manner, but soon arrested on the right-hand side at 23 min while continuing unilaterally from the left before ultimately halting and completely regressing (Fig. 5, 35–52 min). Few interior MT bundles were detected in this cell and those appeared to rapidly degrade. In contrast to wild-type cells, which consistently formed stable interior central spindles ($n = 11$), we observed stable interior MTs in only 7/15 (47%) of the mutant cells filmed. These data indicate that *orbit* mutant cells display defects in central spindle formation, correlating with a failure of cytokinesis. The interior central spindle MTs are more severely affected than those of the periphery and furrows initiate but then may regress and fail.

Interior central spindle MTs fail to release from the spindle poles in *orbit* mutants

Our observations of wild-type cells indicated that at least two events are involved in the formation of the interior central spindle: the release of a subset of elongating MTs from the spindle poles and the overlapping of their plus ends for subsequent bundling. The former event is also evident when spermatocytes are stained to reveal the putative MT minus end binding protein Asp (Riparbelli et al., 2002). In wild-type telophase cells, Asp localizes to the centrosomes and is also visible along a 2–4- μ m length at the minus ends of MTs that have been released and form the central spindle (Fig. 6 A, arrows). In those *orbit* mutant cells where no central spindle formed, Asp remained predominantly at the centrosomes and spindle poles. None was detected in association with the putative interior MTs spanning between the daughter nuclei (Fig. 6 B, arrowheads). When central spindle structures (i.e., bundles that were not pole associated)

were apparent, the MT bundles tended to be on the periphery of cells and in such cases Asp was seen on the predicted minus ends (Fig. 6 B, arrow). These data indicate that *orbit* mutants preferentially fail to release interior MTs from the spindle poles concomitant with central spindle formation.

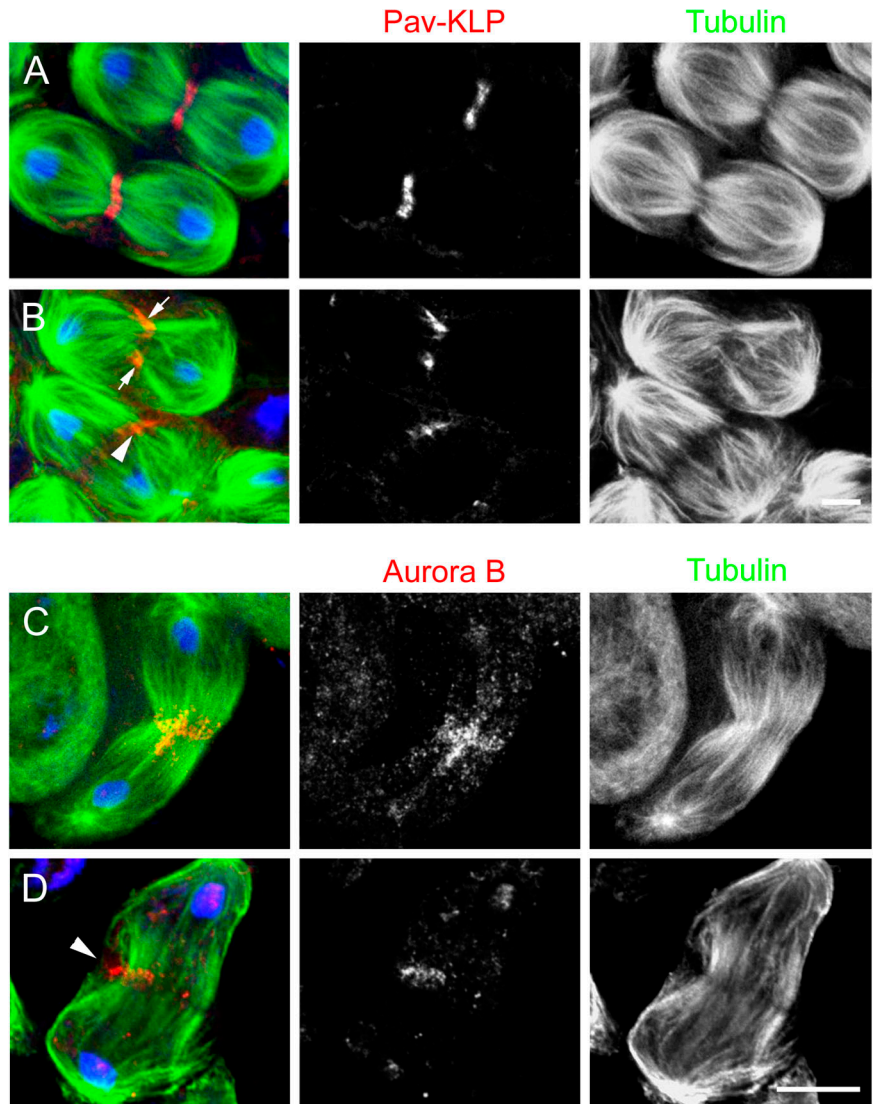
orbit mutants do not recruit Pav-KLP or aurora B to interior central spindle MTs

The lack of discreet bundles in the interior portion of the central spindle lead us to examine the distribution of the kinesin-like protein encoded by *pavarotti* (Pav-KLP; *Zen-4* in *C. elegans* and MKLP1 in mammalian cells). This motor protein associates with putative MT plus ends and is essential for cytokinesis (Adams et al., 1998; Ministrini et al., 2002). In late anaphase/telophase, wild-type spermatocytes, Pav-KLP forms a ring that defines the midpoint of the central spindle (Fig. 7 A). We found three classes of Pav-KLP distribution in *orbit* mutants that coincided with the degree of central spindle development. In the first class, the central spindles appeared normal and Pav-KLP concentrated into an equatorial band. In the second, no central spindles could be discerned and Pav-KLP was also undetectable above background levels. In the third class, Pav-KLP was concentrated on either a single side of the central spindle (Fig. 7 B, arrowhead) or was found on bundles on both sides of the cell but was absent from the intervening space at the predicted interior central spindle location (Fig. 7 B, arrows).

We also investigated the distribution of Aurora B kinase, a member of the INCENP and Survivin complex that has been shown to recruit and possibly activate Pav-KLP/*Zen-4* (Severson et al., 2000; Mishima and Glotzer, 2003). As shown in Fig. 7 C, in wild-type cells, Aurora B formed an

Figure 7. Pavarotti kinesin-like protein (Pav-KLP) and Aurora B kinase fail to accumulate in the interior central spindle at late anaphase in *orbit* mutant spermatocytes.

(A and B) Left panels show late anaphase spermatocytes stained to reveal Pav-KLP (red), MTs (green), and DNA (blue). (A) In wild-type cells, Pav-KLP forms a distinct band at the mid-portion of the central spindle. (B) Partial formation of central spindles in the *orbit* mutant resulted in some accumulation of Pav-KLP where putative plus ends of peripheral central spindle MTs interdigitate near the cell cortex. In some cells this was asymmetric (arrowhead), whereas in others it was on either side of a MT gap (arrows). (C and D) Aurora B kinase also mislocalizes in *orbit* mutants. Aurora B is shown in red, MTs are stained green, and DNA blue. Similar to Pav-KLP, Aurora B assumes a tight ring-like configuration at the equator of wild-type cells (A). This distribution is less symmetrical in mutants, in which the protein could accumulate most strongly at the regions where the peripheral MTs overlapped (B, arrowhead). Bars: (B) 5 μm ; (D) 10 μm .



equatorial band similar to that of Pav-KLP. In contrast, in *orbit* mutants, Aurora B often assumed an asymmetrical localization across the central spindle (Fig. 7 D, arrowhead) or was undetectable above background levels. Thus, in *orbit* mutants, the interior MTs are preferentially affected and fail to form bundles and to recruit Pav-KLP and Aurora B.

Both anillin and actin rings may fail to form in *orbit* mutants

The aforementioned data indicated that a principal consequence of the *orbit* mutation was a failure to properly form and/or maintain interior central spindles. To further characterize how loss of this structure affected cytokinesis, we examined the distribution of other cleavage furrow-associated proteins. We began our analysis by looking at the distribution of anillin, an actin-binding protein that is recruited to a narrow band around the cell equator before the formation of the actin contractile ring (Giansanti et al., 1999). In wild-type cells, anillin formed an equatorial ring as early as anaphase, where it remained as the furrow ingressed (Fig. 8 A). Giansanti et al. (1999) found that anillin localization was unperturbed even after the central spindle was disrupted us-

ing two separate mutants, *chickadee* and *klp3A*. Therefore, we were surprised to find that anillin was only weakly recruited to the equator of *orbit* spermatocytes at anaphase. When anillin did form discrete structures, they tended to be aggregates concentrated along one side of the cortex in the region occupied by peripheral central spindle MTs (Fig. 8 B, arrowhead). After anillin accumulation, the force-generating actomyosin contractile ring forms through a central spindle dependent mechanism (Gatti et al., 2000). Indeed, in wild-type cells we observed clear rings of actin that were concentrated around the equator of the cell in the mid-part of the central spindle (Fig. 8 C). As expected, whenever the interior central spindle was disorganized in *orbit* cells, actin rings were equally aberrant or undetectable (Fig. 8 D, arrowheads).

Discussion

Our study of MT behavior during the early stages of cytokinesis in living *Drosophila* primary spermatocytes has identified two classes of central spindle MTs. The first corresponds to the peripheral MTs of the asters, which dynami-

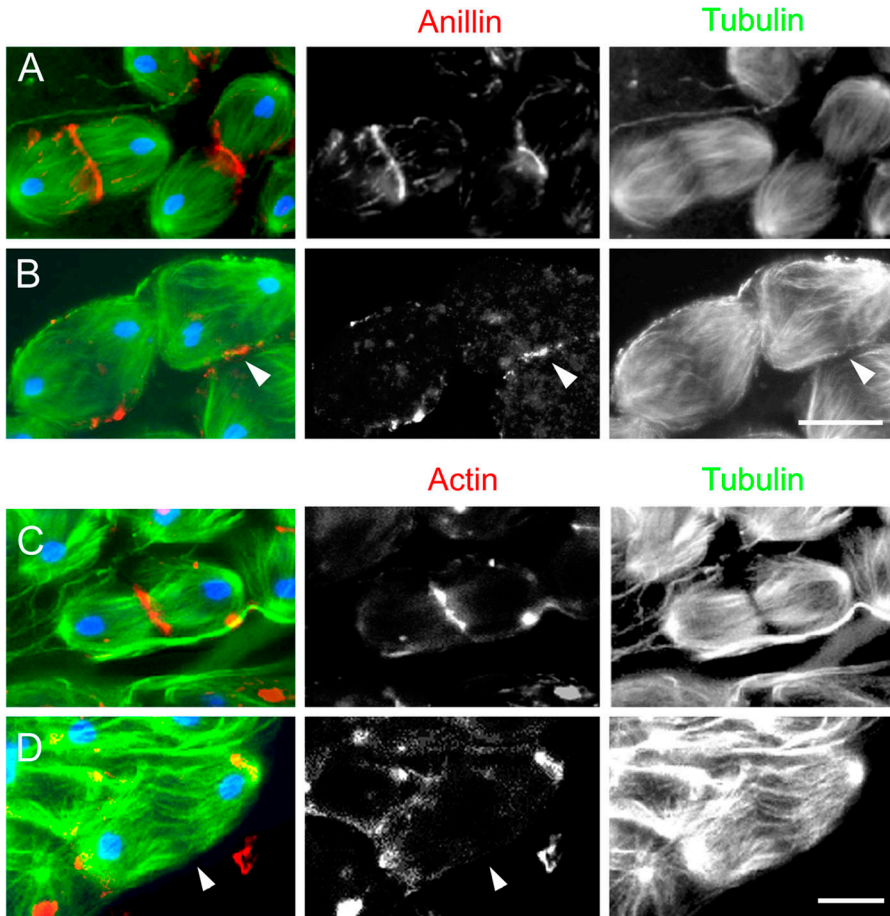


Figure 8. *orbit* mutants do not properly localize anillin or actin. Wild-type testes (A) and *orbit* mutant testes (B) were stained to visualize MTs (green), DNA (blue), and anillin or actin (red). (A) During central spindle formation, wild-type cells concentrate anillin into a band at the future cleavage site. (B) Two cells from a cyst of an *orbit* mutant testis in which an anillin ring failed to properly develop. Anillin does not assume a band-like distribution but is found as cortical aggregates. Some of these appear to associate with the MTs of the peripheral central spindle (arrowhead). Similarly, actin, which forms an equatorial ring on the central spindle in wild-type cells, is poorly organized or fails to accumulate (D, arrowheads) in *orbit* mutants. Bars, 10 μ m.

cally probe the cytoplasm as they extend along the cell periphery. This probing continues until the MTs contact the cortex and bundle at the location of the future cleavage site. These MTs translocate toward the spindle equator and form a series of overlapping bundles, a structure that we term the “peripheral central spindle.” These are distinct from the interior MTs, which are located within the spindle envelope and appear to elongate and then appear to be released from the spindle poles to form the overlapping bundles of the “interior central spindle.” It has been known for some time that cytokinesis in *Drosophila* spermatocytes requires the integrity of the central spindle MTs (Gatti et al., 2000; Giansanti et al., 1998, 2001). However, our present study assigns the peripheral central spindle MTs the role of initiating furrow formation where they contact the equatorial cortex to form bundles, and a second function to the interior central spindle MTs to stabilize and propagate the furrow. In agreement with our findings, recent observations of *Drosophila* primary spermatocytes mutant for the *asp* MT binding protein also implicate astral MTs in furrow placement. In these cells, the asters position themselves independently of an acentrosomally derived spindle. During cytokinesis, furrows initiate at locations between the two asters irrespective of the spindle axis (Rebollo et al., 2004). Along with this functional difference, our data suggest that peripheral and interior MTs are biochemically distinct, as the Orbit/Mast protein strongly accumulated in the region of the putative spindle matrix in the vicinity of the interior MTs,

whereas it was not detectable above background levels on the regions containing the peripheral MTs. We find that interior MTs are preferentially affected in *orbit* mutants and fail to form stable interior central spindles; subsequently, cleavage furrows may initiate but not be sustained, leading to cytokinetic failure.

The bundling of peripheral MTs simultaneous with or shortly after they contact the cortex but before furrowing onset raises the possibility that either of these events could be essential for furrowing. Successful cytokinesis has been shown to correlate with the presence of a central spindle-like structure even in the absence of canonical bipolar spindles. For example, when two spindles share a common cytoplasm in PtK1 cells at anaphase, not only does each spindle develop a mid-zone comprised of overlapping MTs and associated proteins, but similar structures form between the asters of the adjacent spindles (Savoian et al., 1999). Moreover, central spindle-like structures can form from the monopolar spindles that result when either γ -tubulin or an associated protein is mutated in *Drosophila* primary spermatocytes. These pseudo-central spindles contain the characteristic cleavage proteins and are functional, leading to asymmetrical cleavage with polyploid and anucleate daughter cells (Sampaio et al., 2001; Barbosa et al., 2003).

Our live cell analyses of S2 cells expressing GFP-tubulin suggest that contact of peripheral astral MTs with the cortex, rather than their bundling, is required for cleavage furrow positioning and onset. In these cells, long astral MTs

emanating from either a single or the two opposing centrosomes contacted the cleavage site near the time of furrow initiation. Similarly, Canman et al. (2003) found that in cultured mammalian cells induced to form monopolar spindles by treatment with monastral, a subpopulation of stable MTs extends past the chromosomes and contacts the cortex at the site of furrow formation. Together these data suggest that it is the presence of astral MT plus ends and not their overlapping configuration that is critical for furrow placement.

In apparent contradiction to these observations, cleavage can occur in the absence of astral MTs. *Drosophila asterless* mutants form central spindles and cleave, and yet asters were not detected in fixed preparations (Bonaccorsi et al., 1998; Giansanti et al., 2001). Moreover, when the asters were removed from living grasshopper spermatocytes during anaphase by microsurgery, both the now asterless main cell and aster-containing cell derivative underwent cytokinesis (Alsop and Zhang, 2003). A fixed cell study of MT and actin distribution in these “asterless” cells during furrow ingression revealed the presence of cortically associated MT bundles. It would be of interest to directly study how MTs form the central spindle under such asterless conditions in living cells.

These data could be reconciled if both the peripheral/astral and interior MTs were able to deliver the same positive regulatory signal but that the peripheral MTs were more efficient at doing so. Thus, in normal wild-type cells, initially dynamic peripheral/astral MTs would contact the cortex and induce furrowing, while subsequent interactions between the interior MTs and the nascent contractile ring would then stabilize the furrow to allow for its propagation and midbody formation.

A likely candidate for such a positive regulator is “central-spindlin.” This highly conserved complex is comprised of an MKLP1 family member associated with a Rho-family GAP (MgcRacGAP in mammalian cells (Minoshima et al., 2003), CYK-4 in *C. elegans* (Mishima et al., 2002), and RacGAP50C in *Drosophila* (Somers and Saint, 2003)). The NH₂-terminal region of RacGAP50C has also been recently shown to associate with the NH₂ terminus of a conserved RhoGEF that in *Drosophila* is known as Pebble, a protein required to initiate furrow formation (Somers and Saint, 2003). Pebble activates RhoA and may promote actin polymerization and activation of Rho-dependent and Citron kinases (Prokopenko et al., 1999; Tatsumoto et al., 1999; D’Avino et al., 2004). However, this model has been questioned in systems containing dense asters like *C. elegans* embryos and also in mammalian cells where overexpression of the NH₂-terminal domain of the Pebble orthologue, ECT2, causes late defects in cytokinesis (Tatsumoto et al., 1999). Resolution of this issue awaits an understanding of the dynamics of furrow propagation, a process likely to be complex and involve cycles of activation and inactivation of the contractile machinery. In this light it will be of future interest to determine the relative parts played by the Pebble/ECT2 Rho GEF and the Rho-family GAP.

Although the peripheral and interior central spindle MTs share several common features particularly with respect to their association with the centralspindlin complex, the present study reveals some differences. Our data suggest Orbit/Mast may be required to promote growth and stability

specifically of the interior central spindle, which forms where the protein preferentially associates. This adds another function to those already shown for this MAP that in early M-phase is needed to maintain spindle bipolarity and to facilitate chromosome congression along MT plus ends (Inoue et al., 2000; Lemos et al., 2000; Maiato et al., 2002). Those authors proposed that the protein promotes kinetochore fiber stability by facilitating the transition between MT shrinkage and growth at the kinetochore. Orbit/Mast may serve a similar role in stabilizing interior central spindle MTs. The diminution of such a MT-stabilizing protein is consistent with the rapid degradation of the interior MTs. It is unclear if the failure to release MTs from the spindle poles in *orbit* mutants is a direct effect or the result of less stable MT plus ends. We speculate that peripheral MTs may require different dynamic properties than those of the interior to allow them to probe the exceptionally large volume of cytoplasm associated with spermatocytes and establish a furrow initiation site. This speculation raises the possibility that the peripheral MTs might use alternative MAPs to establish their zone of overlap.

Our work sheds new light on the question of whether or not cytokinesis is directed by astral or central spindle MTs. Our observation that peripheral MTs specifically invade the equatorial cortex and become bundled at the site of furrow initiation conflicts with the hypothesis that cytokinesis occurs at regions of low MT density. It is easier to accommodate our observations into a model in which MTs supply a positive regulator of cytokinesis (or a negative regulator of some other inhibitor) rather than providing a means of concentrating inhibitory molecules.

Materials and methods

Fly strains

This study was performed on *orbit*⁷ and *orbit*⁸ flies, which were generated as described in the text. Immunofluorescence was performed on testes isolated from either third instar larvae or pharate adults of the genotypes *orbit*⁷/*orbit*⁷ or *orbit*⁸/*orbit*⁸, both of which gave similar results. Because *orbit*⁸/*orbit*⁸ testes tend to have a higher number of apoptotic cells, flies that were homozygous for both *orbit*⁷ and β -tubulin-EGFP were used for live-cell observations. Canton-S and homozygous β -tubulin-EGFP flies (provided by Y. Akiyama-Oda and H. Oda, JT Biohistory Research Hall, Takatsuki City, Japan) were used as wild-type controls for immunofluorescence and time-lapse studies, respectively. Flies were maintained according to standard procedures.

Live cell imaging

To follow cytokinesis in living primary spermatocytes, we modified our previous protocol (Savoian et al., 2000). We observed our living cells in “open” chambers. These were constructed by adhering clean No. 1 1/2 thickness glass coverslips to the underside of aluminum slides in which the center-most portion had been removed, leaving a depression into which the cells could be placed. Testes were isolated from adult flies and their cells spread under Voltalef 10s oil (Elf Atochem) onto the attached coverslips for subsequent filming. Time-lapse imaging was performed on a microscope (model Axiovert 200; Carl Zeiss MicroImaging, Inc.) outfitted with excitation, emission, and neutral density filterwheels (Prior Scientific) and a PIFOC z-axis focus drive (Physik Instruments). Cells were imaged with a 100 \times (NA 1.4) lens and long working distance DIC condenser (NA 0.55). Specimens were illuminated with heat and UV filtered, shuttered light using the appropriate filter wheel combinations through an EGFP/DsRed filter cube (Chroma Technology Corp.). At each 1 min time interval, six, near-simultaneous fluorescence (EGFP) and transmitted light (DIC) optical sections (1 μ m step size) were captured with a camera (model Cool-snap HQ; Roper Scientific) using a 2 \times 2 bin. Image acquisition was controlled through the Metamorph software package (Universal Imaging

Corp.) running on a PC. To determine fluorescence intensity distributions, maximum intensity projections were analyzed using the linescan function along the length of the spindle as shown in the figures with a line width of 30 pixels. The values were exported into Excel (Microsoft) for plotting before being incorporated into the figures.

Montages were created in Adobe Photoshop®. Each fluorescence image is the maximum intensity projection of the six individual optical sections for that time point. The DIC image is the corresponding, single central section.

Testes squashes to evaluate onion stage spermatids were made using standard protocols and viewed by phase-contrast microscopy.

GFP-tubulin-expressing S2 cells (Goshima and Vale, 2003) were grown on clean No. 1 1/2 coverslips. These were mounted on 65 µl Gene frames (ABgene) filled with complete Schneider's medium directly before filming. Z-series were acquired every 15–30 s on an Ultraview rs spinning disk confocal system attached to a microscope using a 100× (NA 1.3) lens and a 2 × 2 bin. Montages and videos are the maximum intensity projections of z-series.

Immunofluorescence

Samples were fixed according to the method of Cenci et al. (1994) unless otherwise indicated. Antigens were labeled using previously described primary antibodies at the following concentrations: anti-acetylated tubulin, 1:50; anti-Orbit, 1:100; anti-Pav-KLP, 1:200; and anti-Asp, 1:200. For anillin staining, cells were fixed according to Bonaccorsi et al. (2000) and labeled with anti-anillin antibodies (a gift of C. Field, Harvard Medical School, Boston, MA) at 1:200. To determine Aurora B distribution, we used the fixation method of Bonaccorsi et al. (2000). The specimens were then stained with anti-Aurora B antibodies at 1:50. Actin was visualized with fluorescently labelled phalloidin. All secondary antibodies and DNA stains were commercially obtained. Stained specimens were imaged using a confocal laser microscope system (Bio-Rad Laboratories; Olympus).

Online supplemental material

Fig. S1 shows phase-contrast images of *orbit*¹ mutant and β -tubulin-EGFP onion stage spermatids. Fig. S2 is a montage of frames taken from a recording of a GFP-tagged tubulin-expressing S2 cell undergoing cytokinesis. Table S1 compares the frequency of division abnormalities between wild-type, β -tubulin-EGFP-expressing, and mutant onion stage spermatids. Video 1 shows cytokinesis in a living, wild-type primary spermatocyte that is expressing β -tubulin-EGFP. Video 2 illustrates how peripheral astral MTs contact the cortex and bundle at the future cleavage site. Video 3 reveals that astral MTs also contact the cleavage site in S2 cells expressing GFP-tagged tubulin. Video 4 and 5 show that *orbit* mutant primary spermatocytes are unable to form stable interior central spindles leading to cytokinetic failure. Online supplemental material is available at <http://www.jcb.org/cgi/content/full/jcb.200402052/DC1>.

We would like to thank Y. Akiyama-Oda and H. Oda for the kind gifts of fly strains and C. Field for the kind gift of anillin antibodies. We wish to further acknowledge T. Sugimoto for technical assistance and C.A. Savoian for the open culture slides.

This work was supported by Programme Grants from the Medical Research Council and Cancer Research UK. Y.H. Inoue received support from Grants-in-Aid for Scientific Research (A) on Priority Areas (14033224) from the Ministry of Education, Culture, Sports, Science and Technology of Japan.

Submitted: 9 February 2004

Accepted: 27 May 2004

References

- Adams, R.R., A.A. Tavares, A. Salzberg, H.J. Bellen, and D.M. Glover. 1998. *parovroti* encodes a kinesin-like protein required to organize the central spindle and contractile ring for cytokinesis. *Genes Dev.* 12:1483–1494.
- Akhmanova, A., C.C. Hoogenraad, K. Drabek, T. Stepanova, B. Dortland, T. Verkerk, W. Vermeulen, B.M. Burgering, C.I. De Zeeuw, F. Grosveld, and N. Galjart. 2001. Clasps are CLIP-115 and -170 associating proteins involved in the regional regulation of microtubule dynamics in motile fibroblasts. *Cell.* 104:923–935.
- Alsop, G.B., and D. Zhang. 2003. Microtubules are the only structural constituent of the spindle apparatus required for induction of cell cleavage. *J. Cell Biol.* 162:383–390.
- Barbosa, V., M. Gatt, E. Rebollo, C. Gonzalez, and D.M. Glover. 2003. *Drosophila* *ila* *dd4* mutants reveal that gammaTuRC is required to maintain juxtaposed half spindles in spermatocytes. *J. Cell Sci.* 116:929–941.
- Bonaccorsi, S., M.G. Giansanti, and M. Gatti. 1998. Spindle self-organization and cytokinesis during male meiosis in asterless mutants of *Drosophila melanogaster*. *J. Cell Biol.* 142:751–761.
- Bonaccorsi, S., M.G. Giansanti, G. Cenci, and M. Gatti. 2000. Cytological analysis of spermatocytes growth and male meiosis in *Drosophila melanogaster*. In *Drosophila* Protocol. W. Sullivan, M. Ashburner, and R.S. Hawley, editors. Cold Spring Harbor Laboratory Press, Cold Spring Harbor, NY. 87–109.
- Canman, J.C., L.A. Cameron, P.S. Maddox, A. Straight, J.S. Tirnauer, T.J. Mitchison, G. Fang, T.M. Kapoor, and E.D. Salmon. 2003. Determining the position of the cell division plane. *Nature.* 424:1074–1078.
- Cao, L.G., and Y.L. Wang. 1996. Signals from the spindle midzone are required for the stimulation of cytokinesis in cultured epithelial cells. *Mol. Biol. Cell.* 7:225–232.
- Carmena, M., M.G. Riparbelli, G. Ministrini, A.M. Tavares, R. Adams, G. Calaini, and D.M. Glover. 1998. *Drosophila* polo kinase is required for cytokinesis. *J. Cell Biol.* 143:659–671.
- Cenci, G., S. Bonaccorsi, C. Pisano, F. Verni, and M. Gatti. 1994. Chromatin and microtubule organization during premeiotic, meiotic and early postmeiotic stages of *Drosophila melanogaster* spermatogenesis. *J. Cell Sci.* 107:3521–3534.
- D'Avino, P.P., M.S. Savoian, and D.M. Glover. 2004. Mutations in sticky lead to defective organization of the contractile ring during cytokinesis and are enhanced by Rho and suppressed by Rac. *J. Cell Biol.* 166:61–71.
- Dechant, R., and M. Glotzer. 2003. Centrosome separation and central spindle assembly act in redundant pathways that regulate microtubule density and trigger cleavage furrow formation. *Dev. Cell.* 4:333–344.
- Eckley, D.M., A.M. Ainsztein, A.M. Mackay, I.G. Goldberg, and W.C. Earnshaw. 1997. Chromosomal proteins and cytokinesis: patterns of cleavage furrow formation and inner centromere protein positioning in mitotic heterokaryons and mid-anaphase cells. *J. Cell Biol.* 136:1169–1183.
- Field, C., R. Li, and K. Oegema. 1999. Cytokinesis in eukaryotes: a mechanistic comparison. *Curr. Opin. Cell Biol.* 11:68–80.
- Gatti, M., M.G. Giansanti, and S. Bonaccorsi. 2000. Relationships between the central spindle and the contractile ring during cytokinesis in animal cells. *Microsc. Res. Tech.* 49:202–288.
- Giansanti, M.G., S. Bonaccorsi, B. Williams, E.V. Williams, C. Santolamazza, M.L. Goldberg, and M. Gatti. 1998. Cooperative interactions between the central spindle and the contractile ring during *Drosophila* cytokinesis. *Genes Dev.* 12:396–410.
- Giansanti, M.G., S. Bonaccorsi, and M. Gatti. 1999. The role of anillin in meiotic cytokinesis of *Drosophila* males. *J. Cell Sci.* 112:2323–2334.
- Giansanti, M.G., M. Gatti, and S. Bonaccorsi. 2001. The role of centrosomes and astral microtubules during asymmetric division of *Drosophila* neuroblasts. *Development.* 128:1137–1145.
- Goshima, G., and R.D. Vale. 2003. The roles of microtubule-based motor proteins in mitosis: comprehensive RNAi analysis in the *Drosophila* S2 line. *J. Cell Biol.* 162:1003–1016.
- Inoue, Y.H., M. do Carmo Avides, M. Shiraki, P. Deak, M. Yamaguchi, Y. Nishimoto, A. Matsukage, and D.M. Glover. 2000. Orbit, a novel microtubule-associated protein essential for mitosis in *Drosophila melanogaster*. *J. Cell Biol.* 149:153–166.
- Jantsch-Plunger, V., P. Gonczy, A. Romano, H. Schnabel, D. Hamill, R. Schnabel, A.A. Hyman, and M. Glotzer. 2000. CYK-4: A Rho family gtpase activating protein (GAP) required for central spindle formation and cytokinesis. *J. Cell Biol.* 149:1391–1404.
- Lemos, C.L., P. Sampaio, H. Maiato, M. Costa, L.V. Omel'yanchuk, V. Liberal, and C.E. Sunkel. 2000. Mast, a conserved microtubule-associated protein required for bipolar mitotic spindle organization. *EMBO J.* 19:3668–3682.
- Maiato, H., P. Sampaio, C.L. Lemos, J. Findlay, M. Carmena, W.C. Earnshaw, and C.E. Sunkel. 2002. MAST/Orbit has a role in microtubule-kinetochore attachment and is essential for chromosome alignment and maintenance of spindle bipolarity. *J. Cell Biol.* 157:749–760.
- Maiato, H., E.A. Fairley, C.L. Rieder, J.R. Swedlow, C.E. Sunkel, and W.C. Earnshaw. 2003. Human CLASP1 is an outer kinetochore component that regulates spindle microtubule dynamics. *Cell.* 113:891–904.
- Máthé, E., Y.H. Inoue, W. Palframan, G. Brown, and D.M. Glover. 2003. Orbit/Mast, the CLASP orthologue of *Drosophila*, is required for asymmetric stem cell and cystocyte divisions and development of the polarised microtubule network that interconnects oocyte and nurse cells during oogenesis. *Development.* 130:901–915.
- Ministrini, G.F., E. Máthé, and D.M. Glover. 2002. Domains of the Pavarotti ki-

- nesin-like protein that direct its subcellular distribution: effects of mislocalisation on the tubulin and actin cytoskeleton during *Drosophila* oogenesis. *J. Cell Sci.* 115:725–736.
- Minoshima, Y., T. Kawashima, K. Hirose, Y. Tonozuka, A. Kawajiri, Y.C. Bao, X. Deng, M. Tatsuka, S. Narumiya, W.S. May Jr., et al. 2003. Phosphorylation by aurora B converts MgcRacGAP to a RhoGAP during cytokinesis. *Dev. Cell.* 4:549–560.
- Mishima, M., and M. Glotzer. 2003. Cytokinesis: a logical GAP. *Curr. Biol.* 13: R589–R591.
- Mishima, M., S. Kaitna, and M. Glotzer. 2002. Central spindle assembly and cytokinesis require a kinesin-like protein/RhoGAP complex with microtubule bundling activity. *Dev. Cell.* 2:41–54.
- Powers, J., O. Bossinger, D. Rose, S. Strome, and W. Saxton. 1998. A nematode kinesin required for cleavage furrow advancement. *Curr. Biol.* 8:1133–1136.
- Prokopenko, S.N., A. Brumby, L. O’Keefe, L. Prior, Y. He, R. Saint and H.J. Bellen. 1999. A putative exchange factor for Rho1 GTPase is required for initiation of cytokinesis in *Drosophila*. *Genes Dev.* 13:2301–2314.
- Raich, W.B., A.N. Moran, J.H. Rothman, and J. Hardin. 1998. Cytokinesis and midzone microtubule organization in *Caenorhabditis elegans* require the kinesin-like protein ZEN-4. *Mol. Biol. Cell.* 9:2037–2049.
- Rappaport, R. 1961. Experiments concerning the cleavage stimulus in sand dollar eggs. *J. Exp. Zool.* 148:81–89.
- Rebollo, E., and C. Gonzalez. 2000. Visualizing the spindle checkpoint in *Drosophila* spermatocytes. *EMBO Rep.* 1:65–70.
- Rebollo, E., S. Llamazares, S., J. Reina, and C. Gonzalez. 2004. Contribution of noncentrosomal microtubules to spindle assembly in *Drosophila* spermatocytes. *PLoS Biol.* 2:54–64.
- Rieder, C.L., A. Khodjakov, L.V. Paliulis, T.M. Fortier, R.W. Cole, and G. Sluder. 1997. Mitosis in vertebrate somatic cells with two spindles: implications for the metaphase/anaphase transition checkpoint and cleavage. *Proc. Natl. Acad. Sci. USA.* 94:5107–5112.
- Riparbelli, M.G., G. Callaini, D.M. Glover, and M.C. Avides. 2002. A requirement for the Abnormal Spindle protein to organise microtubules of the central spindle for cytokinesis in *Drosophila*. *J. Cell Sci.* 115:913–922.
- Sampaio, P., E. Rebollo, H. Varmark, C.E. Sunkel, and C. Gonzalez. 2001. Organized microtubule arrays in gamma-tubulin-depleted *Drosophila* spermatocytes. *Curr. Biol.* 11:1788–1793.
- Satterwhite, L.L., and T.D. Pollard. 1992. Cytokinesis. *Curr. Opin. Cell Biol.* 4:43–52.
- Savoian, M.S., W.C. Earnshaw, A. Khodjakov, and C.L. Rieder. 1999. Cleavage furrows formed between centrosomes lacking an intervening spindle and chromosomes contain microtubule bundles, INCENP, and CHO1 but not CENP-E. *Mol. Biol. Cell.* 10:297–311.
- Savoian, M.S., M.L. Goldberg, and C.L. Rieder. 2000. The rate of poleward chromosome motion is attenuated in *Drosophila zw10* and *rod* mutants. *Nat. Cell Biol.* 2:948–952.
- Scholey, J.M., G.C. Rogers, and D.J. Sharp. 2001. Mitosis, microtubules, and the matrix. *J. Cell Biol.* 154:261–266.
- Severson, A.F., D.R. Hamill, J.C. Carter, J. Schumacher, and B. Bowerman. 2000. The aurora-related kinase AIR-2 recruits ZEN-4/CeMKLP1 to the mitotic spindle at metaphase and is required for cytokinesis. *Curr. Biol.* 10: 1162–1171.
- Somers, W.G., and R. Saint. 2003. A RhoGEF and Rho family GTPase-activating protein complex links the contractile ring to cortical microtubules at the onset of cytokinesis. *Dev. Cell.* 4:29–39.
- Somma, M.P., B. Fasulo, G. Cenci, E. Cundari, and M. Gatti. 2002. Molecular dissection of cytokinesis by RNA interference in *Drosophila* cultured cells. *Mol. Biol. Cell.* 13:2448–2460.
- Stafstrom, J.P., and L.A. Staehelin. 1984. Dynamics of the nuclear envelope and of nuclear pore complexes during mitosis in the *Drosophila* embryo. *Eur. J. Cell Biol.* 34:179–189.
- Tates, A.D. 1971. Cyto-differentiation during spermatogenesis in *Drosophila melanogaster*: An electron microscope study. Ph.D. thesis. Rijksuniversiteit, Leiden, Netherlands. 166 pp.
- Tatsumoto, T., X. Xie, R. Blumenthal, I. Okamoto, and T. Miki. 1999. Human ECT2 is an exchange factor for Rho GTPases, phosphorylated in G2/M phases, and involved in cytokinesis. *J. Cell Biol.* 147:921–928.
- Wakefield, J.G., S. Bonaccorsi, and M. Gatti. 2001. The *Drosophila* protein asp is involved in microtubule organization during spindle formation and cytokinesis. *J. Cell Biol.* 153:637–648.
- Wolpert, L. 1960. The mechanics and mechanism of cleavage. *Int. Rev. Cytol.* 10: 163–216.